Numerical modelling of a turbulent bluff-body flow with Reynolds stress turbulent models*

LI Guoxiu[1**] and Dirk ROEKAERTS[2]

(1. School of Mechanical, Electronic and Control Engineering, Beijing Jiaotong University, Beijing 100044, China; 2. Department of Applied Physics, Delft University of Technology, CJ2628 Delft, The Netherlands)

Received August 23, 2004; revised December 1, 2004

Abstract Numerical modelling of a turbulent bluff-body flow has been performed using differential Reynolds stress models (DRSMs). To clarify the applicability of the existing DRSMs in this complex flow, several typical DRSMs, including LRR-IP model, JM model, SSG model, as well as a modified LRR-IP model, have been validated and evaluated. The performance difference between various DRSMs is quite significant. Most of the above mentioned DRSMs cannot provide overall satisfactory predictions for this challenging test case. Motivated by the deficiency of the existing approaches, a new modification of LRR-IP model has been proposed. A very significant improvement of the prediction of flow field is obtained.

Keywords: **bluff-body flow, differential Reynolds stress models, turbulent model.**

A bluff-body stabilized flow has received special attention recently[1—4]. In addition to its practical interest, the bluff-body flow is an excellent challenging test case for turbulence model due to its simple and well defined initial and boundary conditions with the complex recirculating flows.

The bluff-body stabilized flow investigated here was studied experimentally by Dally et al.[1, 2] As for its numerical simulation, Dally et al.[1] reported simulation results obtained using standard and modified k-ε model and Reynolds stress models. They found that a simple modification to the $C_{\varepsilon 1}$ constants in the dissipation equation gave better prediction results in the recirculation zone, but did not lead to any improvement further downstream, especially for rms (root mean square) fluctuating axial and radial velocities. Merci et al.[3] applied a cubic nonlinear eddy viscosity turbulence model to simulate the bluff-body flow. Better prediction results in the recirculation zone were obtained compared with the standard linear models.

So far, a number of differential Reynolds stress models (DRSMs) have been proposed, including the LRR-IP model, the original model of Hanjalic and Launder (HL), the quasi-isotropic model (LRR-QI) of Launder et al., the model proposed by Jones and Musonge (JM), the model of Fu, Launder and Tselepidakis (FLT), the model of Craft and Launder (CL), and the SSG model. A major difference between the various DRSMs is in the treatment of pressure strain term.

Till now, little research has been conducted to numerically investigate the complicated and challenging bluff-body stabilized flow with the above-mentioned DRSMs. Therefore, it is worthwhile to clarify the applicability of the various DRSMs to this complex flow. In the present study, several typical models including the LRR-IP model, JM model, SSG model, as well as a modified LRR-IP model have been applied and evaluated in the bluff-body flow.

1 Turbulence models

In the DRSM model, the Reynolds stresses are calculated from their own transport equations. Assuming high Reynolds number, viscous terms are neglected except for the viscous dissipation term ε_{ij}. The Reynolds stress equation for variable density flows then reads[5]:

$$\bar{\rho}\frac{\mathrm{D}}{\mathrm{D}t}\widetilde{u_i''u_j''} = -\bar{\rho}\,\widetilde{u_i''u_k''}\frac{\partial \tilde{U}_j}{\partial x_k} - \bar{\rho}\,\widetilde{u_j''u_k''}\frac{\partial \tilde{U}_i}{\partial x_k} \quad (1a)$$

$$-\left[\overline{u_i''\frac{\partial p'}{\partial x_j}} + \overline{u_j''\frac{\partial p'}{\partial x_i}} - \frac{2}{3}\delta_{ij}\overline{u_k''\frac{\partial p'}{\partial x_k}}\right] \quad (1b)$$

$$-\bar{\rho}\varepsilon_{ij} \quad (1c)$$

* Supported by National Natural Science Foundation of China (Grant No. 50406003) and the project-sponsored by SRF for ROCS, SEM

** To whom correspondence should be addressed. E-mail: gxli@center.njtu.edu.cn

$$-\frac{\partial}{\partial x_k}\left[\bar{\rho}\,\overline{u_i'' u_j'' u_k''}+\frac{2}{3}\delta_{ij}\overline{u_k'' p'}\right] \quad (1d)$$

$$-\overline{u_i''}\frac{\partial \bar{p}}{\partial x_j}-\overline{u_j''}\frac{\partial \bar{p}}{\partial x_i} \quad (1e)$$

$$+\frac{2}{3}\delta_{ij}\overline{p'\frac{\partial u_k''}{\partial x_k}}. \quad (1f)$$

Here, u_i'', u_j'' and u_k'' are the turbulent fluctuation of the velocity vectors about Reynolds average; U_i and U_j are the mean velocity vectors; p is the pressure and p' is the fluctuation of pressure about Favre-averaged quantities; ρ is the density; and x_i, x_j and x_k are the cartesian space coordinates. The overbar denotes the Reynolds average and the tilde identifies Favre-averaged quantities. An exception to this convention is the triple correlation, where the overbar denotes Favre averaging. The terms on the RHS are: the production term P_{ij} (1a), the pressure-strain correlation Φ_{ij} (1b), the viscous dissipation ε_{ij} (1c), the turbulent flux Γ_{ij} (1d), and two terms which are zero in constant density flows containing a mean pressure gradient (1e), and the trace of the fluctuating strain tensor (1f).

The production term is in a closed form and does not need to be modelled, whereas the pressure-strain correlation, dissipation, turbulent flux, and fluctuating density terms have to be modelled.

The diffusive transport is described by the gradient transport approximation

$$\overline{u_i'' u_j'' u_k''}=-C_s\frac{k}{\varepsilon}u_k'' u_l''\frac{\partial u_i'' u_j''}{\partial x_l}, \quad (2)$$

where $C_s=0.2$, u_l'' is the turbulent fluctuation of the velocity vector about Reynolds-averaged quantities, and k is the turbulent kinetic energy.

The viscous dissipation ε_{ij} is modelled by assuming local isotropy at the smallest scales where viscous dissipation takes place. The dissipation model is then defined as:

$$\varepsilon_{ij}=\frac{2}{3}\varepsilon\delta_{ij}, \quad (3)$$

where δ_{ij} is the kronecker tensor.

The turbulent energy dissipation rate ε is calculated from the following modelled equation:

$$\bar{\rho}\frac{\mathrm{D}}{\mathrm{D}t}\varepsilon=C_\varepsilon\frac{\partial}{\partial x_k}\left[\frac{k}{\varepsilon}u_k'' u_l''\frac{\partial\varepsilon}{\partial x_l}\right]+C_{\varepsilon 1}\frac{\varepsilon}{k}P_k-C_{\varepsilon 2}\bar{\rho}\frac{\varepsilon^2}{k}, \quad (4)$$

where $C_\varepsilon=0.18$, $C_{\varepsilon 1}=1.44$, $C_{\varepsilon 2}=1.92$, and P_k is the production of turbulent kinetic energy by mean shear given by

$$P_k=-\bar{\rho}\,u_i'' u_j''\frac{\partial U_i}{\partial x_j}. \quad (5)$$

The final unclosed term is the pressure-strain correlation term. Generally the pressure-strain correlation Φ_{ij} can be decomposed into a slow part and a rapid part according to the following expression

$$\Phi_{ij}=\Phi_{ij,1}+\Phi_{ij,2}. \quad (6)$$

Generally, the first item $\Phi_{ij,1}$, which is called the slow pressure-strain term, is normally modelled in terms of stress anisotropy tensor and its first and/or second invariants. The second term $\Phi_{ij,2}$ is referred to as the rapid pressure-strain, which can be modelled in terms of the mean rate of strain, mean vorticity and stress anisotropy tensor. The pressure-strain correlation models used in the present study are LRR-IP model, JM model, and SSG model. Detailed information can be found in Ref. [4].

2 Grid and boundary conditions

The computational domain, with the symmetry axis as boundary, is 300 mm long in the axial direction and 150 mm long in the radial direction. The lower boundary of the computational domain is at the height of the downstream face of the bluff body. The computational grid consisting of 160 × 128 cells is stretched in the radial direction as well as the axial direction. Grid independence has been guaranteed.

The boundary conditions are carefully determined as follows. At the jet and co-flow regions of the boundary, the experimental data are used for the axial velocity of the co-flow, and also the profiles of normal Reynolds stresses of the center jet and co-flow are obtained and calculated from the experimental data. The axial velocity in the central jet region, the shear Reynolds stress, and the dissipation rate are all calculated according to the formula provided in Ref. [6]. A no slip boundary condition with standard wall functions is applied at the bluff body face. Symmetry conditions are applied at the symmetry axis.

3 Results and discussions

It is well known that the standard Reynolds stress model overpredicts the decay rate and the spreading rate of the round jet. Despite of a number of complicated modifications, Dally et al.[1] found that, when a constant value of $C_{\varepsilon 1}=1.6$ (denoted as BM-M1) instead of the standard value of 1.44 was used, a very significant improvement was obtained in the calculated results for the round jets, better than any other complicated modifications. However, for the bluff-body flame, except that the decay rate of the centerline velocity is correctly predicted in the recirculation zone, it did not lead to any improvement for rms fluctuating velocities especially further downstream. Motivated by this deficiency, we here propose a new modification of the LRR-IP model. Instead of modifying the model constant $C_{\varepsilon 1}$ in the dissipation equation, we change the model constant C_2 in the pressure-strain model from 0.6 to 0.7. We denote this modification of LRR-IP model as BM-M2. It was found that in this way one could obtain a very pronounced improvement in the prediction of the flow field, not only providing the correct decay rate of velocity on the symmetry axis, but also showing a very significant improvement for the rms fluctuation velocities.

The bluff-body burner investigated here is described in detail in Ref. [1]. The central fuel hole diameter is 3.6 mm and the diameter of the bluff-body (D_b) is 50 mm. The mixing properties of flow have been measured. The jet and the co-flow consist of air and hence the flow has constant density. The bulk velocity of the jet is 61 m/s and the co-flow velocity is 20 m/s.

Here we present and discuss results of the numerical simulations of the bluff-body flow using LRR-IP, JM and SSG and two modifications of LRR-IP model, denoted as BM-M1 and BM-M2. The computational results are presented as radial profiles at different axial locations, and one set of experimental data[7] is also plotted for comparison.

Fig. 1 shows the evolution of the mean axial velocity. A first criterion is the prediction of the length of the recirculation zone behind the bluff body. It is experimentally found that $x/D_b=1.0$[1], which is quite well predicted by the two modified LRR-IP models, as well as the standard LRR-IP model and SSG model. However, JM model fails to predict the length of the recirculation zone.

Prediction of the decay rate of axial velocity on the centreline is another essential test. It can be clearly seen from Fig. 1 that the standard LRR-IP model and JM model considerably overpredicts the decay rate of velocity along the symmetry axis, and the discrepancy is larger further downstream. In contrast, the SSG model gives the better results up to $x/D_b=0.4$, then starts to deviate from the measured trends. On the other hand, it is remarkable that both the modified LRR-IP models, i.e. BM-M1 and BM-M2, show better agreement with the experimental data, not only in the recirculation zone but also further downstream up to $x/D_b=1.4$, and therefore perform much better than the SSG model, the standard LRR-IP model, and JM model.

The mean radial velocity component is not shown here due to space limitation.

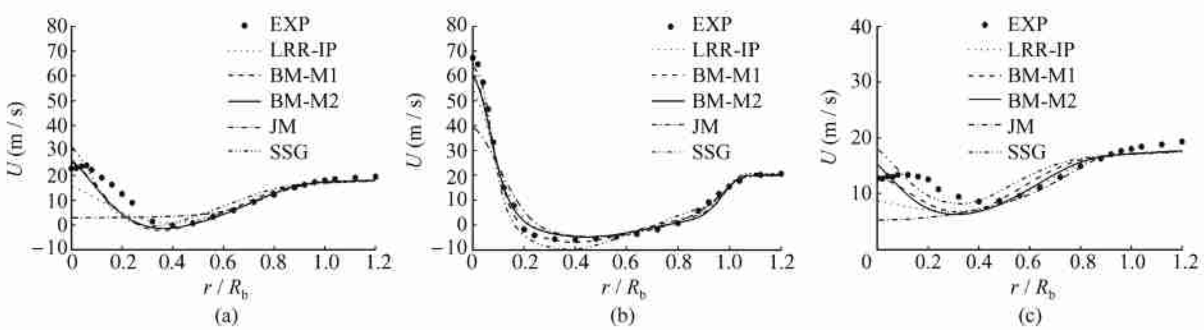

Fig. 1. Radial profiles of mean axial velocity at different axial locations. (a) $x/D_b=0.4$; (b) $x/D_b=1.0$; (c) $x/D_b=1.4$.

Fig. 2 shows the rms fluctuation of axial velocity. It is interesting to see that all of the models show a reasonably good agreement with the experimental data up to $x/D_b=0.4$, and then the performance of the models begins to vary. Near the centreline, the SSG model and BM-M1 model produce better results than those of the standard LRR-IP model and JM model; whereas away from the axis in the region above the bluff-body, the predictions of the standard LRR-IP model (and the JM model) are closest to the experimental data. This can partially be understood as a consequence of the quality of the predictions for the (gradients of) mean velocity that are felt in the rapid part of the pressure strain correlation. (SSG model gives good predictions of mean velocity close to the centreline, while LRR-IP model performs well away from the centreline). Clearly, only BM-M2 yields overall satisfactory results that shows a reasonably good agreement with the experimental data, and also produces a very significant improvement further downstream.

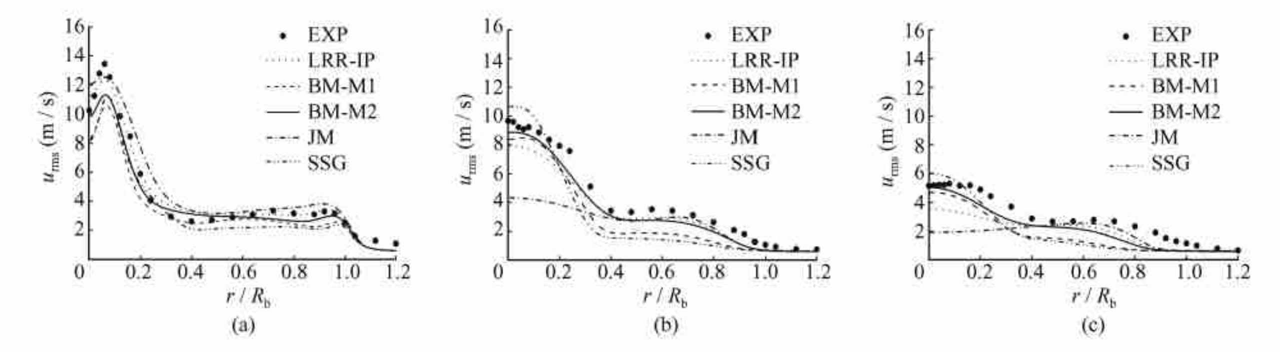

Fig. 2. Radial profiles of rms fluctuation of mean axial velocity at different axial locations. (a) $x/D_b = 0.4$; (b) $x/D_b = 1.0$; (c) $x/D_b = 1.4$.

Fig. 3 shows the rms fluctuation radial velocity, showing a very similar performance of the models to the rms fluctuating axial velocity. Again, the BM-M2 shows best agreement with the experimental data even further downstream and performs much better than any other model.

The predictions of turbulent shear stress are shown in Fig. 4. Near the centreline in the recirculation zone, the SSG model as well as the two modified LRR-IP models can agree well with the experimental data, while the standard LRR-IP model and JM model give a poor prediction. However, in the region above the bluff-body, the standard LRR-IP model and JM model yield results in close agreement with the experimental data even further downstream. But globally, only the BM-M2 provides results at least qualitatively in good agreement with the experimental data.

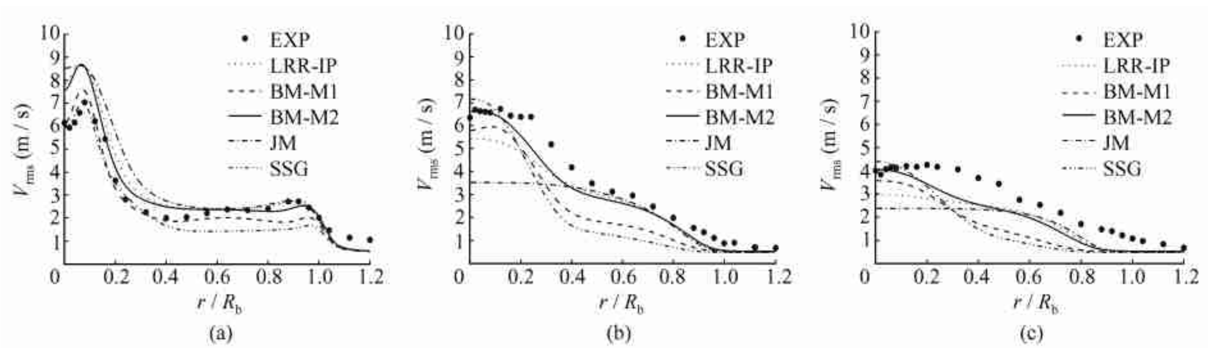

Fig. 3. Radial profiles of rms fluctuation of radial velocity at different axial locations. (a) $x/D_b = 0.4$; (b) $x/D_b = 1.0$; (c) $x/D_b = 1.4$.

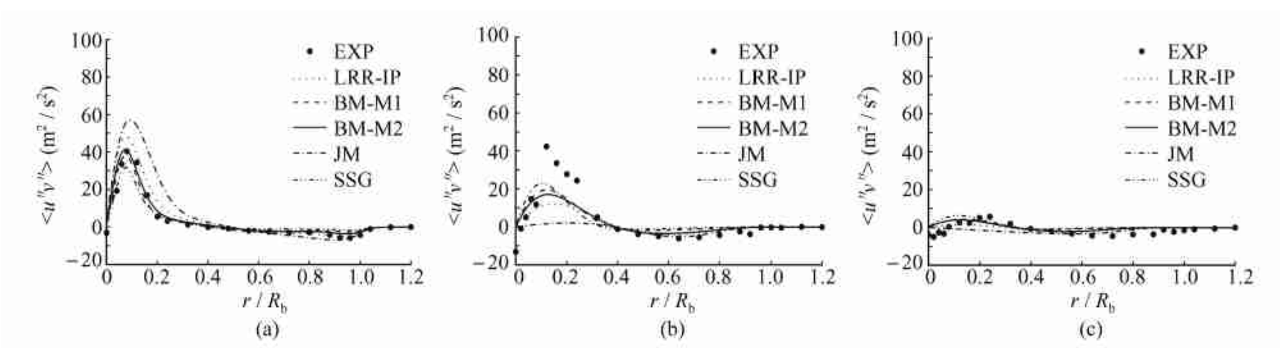

Fig. 4. Radial profiles of turbulent shear stress at different axial locations. (a) $x/D_b = 0.4$; (b) $x/D_b = 1.0$; (c) $x/D_b = 1.4$.

It is worthwhile to observe that, with BM-M2, on the one hand, the predictions near the centreline for the rms fluctuation of velocities are as good as that of BM-M1 model and SSG model; on the other hand, the results in the region over the bluff-body are also pretty well similar to the standard LRR-IP model and JM model. In other words, it appears that BM-M2 combines the advantage of all models, yields the overall satisfactory results, which are in good agreement with the experimental data along the whole axial direction, even further downstream.

4 Conclusions

To clarify the applicability of the various models, three typical DRSMs (LRR-IP, JM, SSG) and two modified versions of the basic LRR-IP model (called BM-M1 and BM-M2) have been applied. It is found that although the JM model is previously demonstrated successful in other flows, it does not perform well in this bluff-body flow. It is also confirmed that the standard LRR-IP model always considerably overpredicts the centreline velocity decay rate, and therefore does not perform well.

In the present study, it is confirmed that a simple modification of LRR-IP model (BM-M1 model) can give better results of axial velocity as well as radial velocity, but it does not lead to improvement for rms fluctuating velocities especially further downstream. Motivated by the need to improve the prediction results, a new modification of the LRR-IP model (i.e. BM-M2 model) has been proposed which can provide overall better predictions compared to the other DRSMs, not only for the axial velocity, but also for the rms fluctuating velocities. With the BM-M2, a very significant improvement of the prediction of flow field is obtained.

References

1 Dally B. B., Fletcher D. F. and Masri A. R. Flow and mixing fields of turbulent bluff-body jets and flames. Combust. Theory Modelling, 1998, 2: 193—219.
2 Dally B. B., Masri A. R., Barlow R. S. et al. Instantaneous and mean compositional structure of bluff-body stabilized nonpremixed flame. Combust. Flame, 1998, 114: 119—148.
3 Merci B., Roekaerts D., Peeters T. W. J. et al. Application of a new cubic turbulence model to piloted and bluff-body diffusion flames. Combust. Flame, 2001, 126: 1533—1556.
4 Li G.-X, Roekaerts D. and Naud B. Numerical investigation of a bluff-body stabilized nonpremixed turbulent flame with differential Reynolds stress model. Flow, Turbulence and Combustion, 2003, 70: 211—240.
5 Roekaerts D. Reacting flows and probability density function methods. In: Closure Strategies for Turbulent and Transitional Flows. Cambridge University Press, Cambridge, 2002, 328—340.
6 Jenny P., Pope S. B., Muradoglu M. et al. PDF simulations of a bluff-body stabilized flow. J. Comp. Phys., 2001, 166: 1—23.
7 Masri A. R. http://www.mech.eng.usyd.edu.au/research/energy/resourses.html. the University of Sydney, dataset HM1E.